

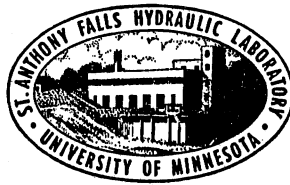
UNIVERSITY OF MINNESOTA
ST. ANTHONY FALLS HYDRAULIC LABORATORY

Project Report No. 236

ANALYSIS OF A HYDROACOUSTIC GRAVITY FLOW FACILITY

by

R.E.A. Arndt, J. M. Wetzel,
D. W. Bintz, and J. F. Ripken



Prepared for

DAVID TAYLOR NAVAL SHIP RESEARCH AND DEVELOPMENT CENTER
Bethesda, Maryland

September, 1984
Minneapolis, Minnesota

University of Minnesota
St. Anthony Falls Hydraulic Laboratory

Project Report No. 236

ANALYSIS OF A HYDROACOUSTIC GRAVITY FLOW FACILITY

by

R.E.A. Arndt, J. M. Wetzel,
D. W. Bintz, and J. F. Ripken

Prepared for

DAVID TAYLOR NAVAL SHIP RESEARCH AND DEVELOPMENT CENTER
Bethesda, Maryland

September, 1984

TABLE OF CONTENTS

	<u>Page No.</u>
I. Introduction	1
II. Preliminary Analysis of Proposed Design	2
A. General Comments	2
B. Estimate of Head Loss	3
1. Local loss coefficient	4
2. Normalization of loss coefficient to test section velocity	10
C. Establishment of Flow in the Alternate Design of the Gravity Flow Facility	10
D. Test Section Boundary Layer Growth	13
E. Test Section Pressures	14
F. Turbulence Management in the Gravity Flow Facility..	14
G. Suggested Component Modifications	17
1. Contraction	17
2. Diffuser Transition	17
III. Alternate Configuration	18
A. Head Tank	18
B. Test Section	18
C. Entrance Contraction	19
D. Downstream Diffuser	19
E. Controller and Head Dissipator	19
F. Short Diffuser	19
G. Vaned Elbow	20
H. Pump Discharge Line	20
I. Pump Diffuser	20
J. Refill Pump	20
References	32

LIST OF FIGURES

Figure No.

- 1 Hydroacoustic gravity flow facility for ship silencing laboratory with sound-absorbing corner vane systems. November 26, 1982, George F. Wislicenus.
- 2 Alternate gravity flow facility design.
- 3 Definition of flow regions in the gravity flow facility.
- 4 Loss coefficient k for square cross-section bends. From Miller [1], Fig. 3.2.2.
- 5 Pressure recoveries - rectangular diffuser ($AR = 2$, $L/D_1 = 30$)-free discharge. from Miller [1], Fig. 61.
- 6 Variation of test section diameter to maintain constant axial velocity.
- 7 Boundary layer displacement thickness and average axial velocity in gravity flow facility with constant test section cross-sectional area.
- 8 Ratios of exit to initial turbulence intensities for different contraction ratios, c . From Ramjee and Hussain [6].
- 9 Isoreduction contours as a function of pressure-drop coefficient and ratio of integral scale of initial turbulence to cell length. From Lumley and McMahon [9].
- 10 Pressure-drop coefficient and length Reynolds number as a function of diameter Reynolds number and length-to-diameter Reynolds number and length-to-diameter ratio. Flow is fully developed above and to the right of the dashed line. From Lumley and McMahon [9].
- 11 Proposed revision of hydroacoustic facility.
- 12 The screen diffuser configuration (all dimensions relate to prototype inside flow surfaces). Taken from SAFHL External Memorandum M-134.

I. INTRODUCTION

Two preliminary designs of a hydroacoustic gravity flow facility have been developed for a Ship Silencing Laboratory, DTNSRDC, by Dr. George F. Wislicenus. It was desired to attain a test section velocity of 60 fps for a 90 sec time period. As the facility will be used for acoustic measurements, cavitation-free flow is a necessity. After a test run has been completed, the water is returned by a pump in a separate line back to the head tank. To maximize usage of the facility, the recycling time between runs should be kept short.

As part of the overall development program, the Laboratory has been asked to carry out some preliminary calculations on the proposed designs to further establish feasibility and to independently evaluate the designs. The calculations included an estimate of head loss in the system and an elementary transient analysis. An alternate configuration also has been suggested for consideration.

II. PRELIMINARY ANALYSIS OF PROPOSED DESIGN

A. General Comments

The sketches for the preliminary designs were reviewed. On the basis of this review, some overall comments with reference to Figs. 1 and 2 are listed in the following:

1. The test section shown in Fig. 1 is so long (27 diameters) that the axial pressure gradient in the test section will vary widely from end to end as will the velocity profiles. This may be considered normal and desirable for some test studies. However, for more conventional water tunnel studies this length is kept short to minimize axial changes in the test region or the test section diameter is made to gradually increase to preserve a near-zero axial pressure gradient. Is the very long cylinder shown in Fig. 1 the form which really best answers the projected test needs?
2. The contraction ahead of the test section should have a smooth "S" shaped profile without the sharp break at the upstream end as shown. The "S" profile can provide a boundary pressure profile essentially free of the adverse pressure gradients which promote boundary layer separation, turbulence and noise.
3. The stilling lengths between the trailing edge of the turning vanes and the leading edge of the honeycomb and between the trailing edge of the honeycomb and the beginning of the contraction may be somewhat short. More length could provide for more decay of the wakes from the turning vanes and honeycomb elements.
4. The cross section of the vaned elbow is rectangular in shape. It is recommended that this be maintained circular in cross section between the circular head tank and the circular contraction cone. If not axial, vortices will form in the corners of the rectangle and these will probably trail well into the test section. These are not only a potentially serious noise source but also form serious perturbations in the uniformity of the test section velocity field. The use of a circular cross section complicates the fabrication of the elbow vaning but should be considered.
5. The boundary at the downstream end of the test section should be fitted with a generous transition curve in passing into the conical diffuser. Separation of flow may otherwise occur here with resultant high turbulence and possibly even cavitation.
6. Figure 1 refers to "sound absorbing corner vane systems." It is unclear whether sound absorption is to be achieved with vane materials which enhance absorption or whether the vane passage configuration is

to attenuate the noise. Unless the professed noise absorbing characteristics are clearly established, it may be worthwhile to consider a form of mitered vane elbow which is simpler and less costly.

7. It is highly desirable that the "turn-around" time between successive tests in the facility be as brief as possible. This means that the turbulence generated in the tank filling cycle should be of as small a scale as possible in order to minimize the eddy decay time. In the proposed drawing the inflow to the storage tank appears to employ a peripheral jet of 94 foot length and one foot depth. This jet has a velocity of about one foot per second during filling and will generate large eddies having relatively long decay time before tests can proceed. Other inflow configurations should be considered. An alternate configuration is offered in a separate section.
8. The reasoning behind the tall downstream tank in Fig. 1 is not apparent. It would appear that this configuration was abandoned and replaced by the configuration of the second drawing, Fig. 2, which includes no such tank. The second form should permit a simpler control for constancy of the test velocity.
9. The roof structure of the head tank should provide atmospheric venting of a size and form which will prevent air whistling.
10. The flow velocity control shown in the second drawing, Fig. 2, is presumed to depend mainly on tubes or slots which provide programmed control of the area of the sheared boundaries involved. There is insufficient detail provided to permit an evaluation. It is an interesting concept. Material costs for the viscous configuration would undoubtedly be high as some 4300 cubic feet of the material is involved. This material must be strong and durable. Plugging by water borne solids may be a serious consideration for the passage sizes that may be required to dissipate the pressure head of 60+ feet. The control valve must be quiet and requires additional investigation.

B. Estimate of Head Loss

The head loss of various components have been estimated, assuming that the loss coefficients do not change with velocity. Interaction effects between components have not been considered. The specific components or regions are indicated in Fig. 3 by Roman numerals.

The following computation will be broken down into two sections: (1) local loss coefficient (k) for each flow region, and (2) normalization of local loss coefficients to test section velocity.

As seen in Figure 5, the flow region (indicated by roman numerals) are:

<u>Region</u>	<u>Description</u>
I	Head Tank
II	Head Tank Transition
III	Head Tank Honeycomb
IV	Elbow #1
V	Turbulence Management Honeycomb
VI	Contraction
VII	Test Section
VIII	Diffuser
IX	Elbow #2
X	Discharge Bell
XI	Tail Tank Honeycomb
XII	Tail Tank

The control valve has a variable head loss factor, since it is this variable that controls the flow rate in the test section. As the loss of the control valve is reduced by opening, the flow rate increases, and correspondingly the flow rate decreases as the control valve is closed to increase headloss through it.

The head loss for each component is defined as $h_L = kV^2/2g$ where V is the appropriate local velocity.

1. Local loss coefficients

a. Head tank, Region I

Velocities will be so small in the head tank that the losses may be neglected. Therefore

$$k \approx 0$$

b. Head tank transition, Region II

As with the head tank, the losses were neglected.

$$k \approx 0$$

c. Head tank honeycomb, Region III

Since the foundation of turbulence reduction is the transfer of eddy energy to friction losses, the k value becomes an important factor. Since no specifics have been established on the dimension of this honeycomb

(or any other) the loss coefficient utilized will be based upon engineering judgement. Generally honeycombs that must greatly reduce incoming turbulence will have a headloss factor between 1 and 4. Since the purpose of this honeycomb is more likely to be for flow straightening rather than turbulence reduction, it is recommended that a low value be selected, since flow straightening does not require the transfer of energy. Therefore, the value for the head loss factor will be assumed as

$$k \approx 1.0$$

and the cross sectional area at the point of reference average velocity (the entrance to the honeycomb) is

$$A_{III} = 18 \text{ ft} \times 18 \text{ ft} = 324 \text{ ft}^2$$

d. Elbow No. 1, Region IV

Due to the relatively large distance between guide vanes along with the long length, this elbow could be expected to act as a long radius elbow. Utilizing Miller's computation [1]* and applying an $r = 18$ and $h = 18$ to Fig. 4 we get a k factor for a 90° elbow of

$$k = 0.24$$

and an entrance cross sectional area of

$$A_{IV} = 324 \text{ ft}^2$$

e. Turbulence Management Honeycomb, Region V

As discussed with the head tank honeycomb, values of headloss coefficients through honeycombs tend to range from 1 to 4. It is most likely that this will be a fine meshed system dictating higher values for headloss. For the first iteration of calculating the total system energy loss, a midrange value will be applied. Later, the sensitivity of the complete facility to the honeycomb cell size can be determined. Therefore

$$k \approx 2.5$$

and the cross-sectional area is

$$A_V = 324 \text{ ft}^2$$

*Numbers in brackets refer to references on page 32.

f. Contraction, Region VI

As a detailed design of the contraction has not been completed, the solution of a loss coefficient is rather arbitrary. Based on previous studies [2], it will be assumed that

$$k \approx 0.02$$

and the reference velocity is the average velocity at the exit of the contraction, where the area is

$$A_{VI} = 3.976 \text{ ft}^2$$

g. Test Section, Region VII

Since this conduit flow will more closely resemble flat plate flow than fully developed pipe flow, the loss coefficient derived for the test section will be related to the friction losses incurred by a flat plate of a width equal to the inner circumference of the test section and a length equal to the test section length. To provide a conservative value for the loss coefficient, a turbulent boundary layer will be assumed. Such an assumption is reasonable, since the flat plate Reynolds number

$$R_\ell = \frac{U\ell}{\nu}$$

(where U = free stream velocity, ℓ = length of plate, and ν = kinematic viscosity) is 2.55×10^8 at design velocity; well into the turbulence zone of the well known resistance diagram for flat plates (Fig. 21.2 of [3]). Further utilizing Schlichting's equation, the drag coefficient is

$$C_D = \frac{0.455}{(\log R_\ell)^{2.58}} = 1.87 \times 10^{-3}$$

This drag coefficient gives a total friction loss of

$$\text{Drag} = C_D b \ell \frac{\rho U^2}{2}$$

where b = plate width, since, by definition,

$$k = H_L / \left(\frac{U^2}{2g} \right)$$

and $H_L = (\text{Drag}/\text{cross-sectional area})(1/\gamma)$

then, with $b = 2.25 \pi$ ft, $l = 60$ ft, $\rho = 1.44$ slugs/ft³,

$$k = \frac{C_D b l \frac{\rho U^2}{2} / (2.25)^2 \frac{\pi}{4}}{\frac{U^2}{2g} \gamma}$$

$$k = C_D (60) (4/2.25)$$

$$k = 0.20$$

This value is based on a drag coefficient calculated for the maximum velocity. The drag coefficient varies as velocity to the minus 0.258 power.

For comparison, the k factor for fully developed pipe flow would be (utilizing the Moody diagram)

$$k = 0.29$$

However, as previously stated, this is not an accurate appraisal of the headloss mechanism in the test section. So, the recommended loss coefficient is

$$k \approx 0.20$$

and the reference cross section area is

$$A_{VII} = (2.25)^2 \pi/4 = 3.976 \text{ ft}^2$$

h. Diffuser, Region VIII

Since this diffuser has a section of straight conduit (constant cross-sectional area) attached to its outlet, we can apply Idel'chik's studies [4] to determine a loss coefficient.

As discussed by Miller [1], the loss coefficient for a diffuser with a tailpipe is the difference between the ideal pressure recovery coefficient, C_1 , and the static pressure coefficient C_p . The ideal pressure recovery coefficient is defined as

$$C_p = 1 - \frac{1}{(AR)^2}$$

where $AR =$ area ratio. Thus,

$$k = C_{p_i} - C_p = 1 - \frac{1}{(AR)^2} - C_p = 0.996 - C_p$$

for an area ratio of 16. Taking a conservative value for the head loss coefficient from the graphs presented in reference [4] for a nonuniform velocity distribution (again being conservative) and a 5° diffusion angle, we get a value of

$$k = 0.126$$

Similarly, data obtained from McDonald and Fox [5] establish a pressure recovery coefficient of $C_p = 0.857$. Utilizing the proper relationship between C_p and k , the value of k is

$$k = 0.139$$

Averaging the results of the above two studies, we get

$$k \approx 0.133$$

This value is associated with the average inlet velocity of the diffuser, where the cross-sectional area is

$$A_{VIII} = 3.976 \text{ ft}^2$$

1. Elbow No. 2, Region IX

Since this elbow is not only an elbow, but also has some diffusion in the later portion of the unit, the headloss will be approximated as the sum of the long radius elbow loss and the diffusion losses.

For the long radius turn segment, the same derivation applies as with elbow No. 1, with equal result, that is:

$$k \approx 0.24$$

With regard to the diffusion portion, Miller's results [1, p. 135] in Fig. 5, utilizing a $W_1 = 9/4$ ft, $W_2 = 11.75/4$ ft and $N = 7$ ft, and an $Re = 6 \times 10^5$ ($= (60 \text{ fps}/16)(9/4)/\nu$) we get a $C_p = 0.7$ ($\theta = 3^\circ$, use 4° curve). And, as discussed by Miller, for a diffuser with a free discharge (which is applicable)

$$k = 1 - C_p$$

Therefore,

$$k = 1 - 0.7 = 0.30$$

Summing up the loss coefficients for the turn of this elbow and the diffusion that follows, the overall headloss coefficient is

$$k \approx 0.54$$

with a cross-sectional area at the point of reference velocity equal to

$$A_{IX} = 9 \text{ ft} \times 9 \text{ ft} = 81 \text{ ft}^2$$

j. Discharge Bell, Region X

This bell was approximated for headloss computations as a set of four short radius elbows. Additional drawings supplied by the designer actually show this discharge as four separate segments directed orthogonally from each other, with honeycomb and high impedance trim attached to the end of the discharge (see Fig. 2). The headloss coefficient was approximated as the sum of the losses through a short radius elbow and losses through a fine mesh honeycomb.

For the short radius elbow loss, again Miller's [1] results were utilized. In the application of Fig. 4 of Ref. (1), the elbow in the discharge bell is approximated as square, with a radius (r) of 10 ft and a height (h) of 8 ft. Entering this figure with turning angle of 90°, the loss coefficient, k is 0.18.

The loss for the turn is expected to be minor in comparison to the estimated losses due to the impedance trim and honeycomb. As previously discussed, no details of the latter have been supplied. A representative loss coefficient for fine mesh honeycomb was selected as k = 2.5.

Therefore, the total headloss coefficient for this discharge bell is

$$k \approx 2.5 + 0.18$$

$$k \approx 2.7$$

and the cross-sectional area that should represent this headloss factor should reflect more the corresponding value of velocity related to the honeycomb (which is the honeycomb entrance velocity) than any representative velocities with respect to the elbow due to the overwhelming predominance of the honeycomb headloss factor. In that regard, the representative area for the discharge bell will then be

$$A_X = 8 \text{ ft} \times 11 \text{ ft} = 88 \text{ ft}^2.$$

k. Tail Tank Honeycomb, Region XI

It is speculated that this honeycomb is nothing more than an acoustic grid, with relatively low levels of frictional energy loss. Therefore, a moderately low headloss coefficient will be assigned for the first iteration ,

$$k \approx 1.0.$$

The representative cross-sectional area is the area of the tail tank minus the area occupied by Elbow No. 2, or

$$A_{XI} = \left(\frac{36}{2} \right)^2 \pi - (10 \times 18.5) = 832 \text{ ft}^2$$

1. Tail Tank, Region XII

Velocities here are so low that it may be assumed that the headloss is negligible and therefore

$$k \approx 0$$

2. Normalization of Loss Coefficient to Test Section Velocity

Since the loss coefficients are based on the local velocity head, normalization of the coefficients to another velocity is simply conducted by multiplication of the factor by the square ratio of the representative velocities. In this case (a closed system), the velocity ratio is equal to the area ratios. The following table establishes these normalized coefficients based on the test section velocity head. The sum of all the normalized coefficients can be applied to the selected test section velocity to determine the minor losses throughout the complete system (see Table 1).

In summary, losses through the facility, from the head tank free surface to the tail tank free surface, are equal to 0.36 times the test section velocity head plus the variable headloss coefficient of the control valve multiplied by the test section velocity head:

$$H = (k_v + 0.36) \frac{V^2}{2g}$$

H = height difference between the head tank free surface and tail tank free surface, k_v = variable loss coefficient of the control valve, and V = test section average velocity.

It should be emphasized that the headloss evaluation is only approximate in this preliminary analysis, and the values of loss coefficients should be verified by experimental measurements in a model study.

C. Establishment of Flow in the Alternate Design of the Gravity Flow Facility

In calculating the time transient flow characteristics of the second generation design for the gravity flow facility (Fig. 2) the following assumptions for the operation of the system were assumed:

(1) During the initial period of flow, when the test section velocity is increasing to 60 fps, variable head losses at the exit bell are minimized in order to reach the desired velocity in the test section as soon as possible. With the exit losses minimized, the only significant losses take place in the contraction, test section, and diffuser. The headloss factor computed for the first generation

TABLE 1 - SUMMARY OF LOSS COEFFICIENTS

Flow Region*	Local Loss Coefficient	Representative Area , ft ²	$(\frac{A_{VII}}{Area})^2$	Normalized Loss Coefficient
I	0	NA	NA	0
II	0	NA	NA	0
III	1.0	324	1.51×10^{-4}	1.51×10^{-4}
IV	0.24	324	1.51×10^{-4}	3.61×10^{-5}
V	2.5	324	1.51×10^{-4}	3.76×10^{-4}
VI	0.02	3.976	1	0.02
VII	0.16	3.976	1	0.20
VIII	0.13	3.976	1	0.13
IX	0.54	81	2.41×10^{-3}	1.30×10^{-3}
X	2.7	88	2.04×10^{-3}	5.51×10^{-3}
XI	1.0	832	2.28×10^{-5}	2.28×10^{-5}
XII	0	NA	NA	0

Example: $k_{IX} = 0.54 \times 2.41 \times 10^{-3} = 1.3 \times 10^{-3}$

$\sum k = 0.36$

See Fig. 3

design are valid with a value of 0.36 as applied to the test section velocity head.

(2) Upon establishment of the desired test section velocity, headloss at the exit will be adjusted to maintain the desired velocity for as long as possible with the water available in the head tank. From the moment of established flow until the exhaustion of head tank water, the headloss factor will be some variable greater than or equal to 0.36 as applied to the test section velocity head.

Integration of the Euler equation from the free-surface of the head tank to the free-surface of the tail tank along with a simplification assumption that velocity changes along the direction of travel are insignificant in the segments where control of flow is taking place (test section and diffuser) and inclusion of turbulent shear forces gives the following governing equation:

$$\frac{dV}{dt} = -k \frac{V^2}{2L} + \frac{2g}{L} H$$

where V = test section velocity, k = loss coefficient (> 0.36), L = distance of travel of water molecule, and H = pressure head on the system (variable with time).

Before applying the above equation to a computerized numerical solution, values for k , L , and H had to be established.

(1) Loss coefficient k . As discussed, k will be set at 0.36 during the initial stage of flow until 60 fps is established in the test section. After this period, k will be adjusted to maintain 60 fps in the test section (until the water supply is depleted or 60 fps cannot be maintained due to too low a pressure head in the head tank).

(2) Distance of Travel L . This term equated to the energy consumed in the time rate of change of momentum. Therefore, this length should be the distance of travel of a particle through this system where velocity (and therefore momentum) are great enough to be of significance. This can be considered to consist of the length of the diffuser, test section, and 2/3 of the contraction, resulting in $L = 150$ ft.

(3) Pressure Head H . This of course will be a function of time equating to the difference in the initial head $H_0 = 99$ ft and the reduction of the height of water in the tank head resulting from flow through the test section. Pressure head was determined numerically and simultaneously with the test section velocity.

The computer algorithm proceeded as follows: with the headloss coefficient at its lowest level (0.36) velocity was allowed to increase to 60 fps. Once the desired velocity was achieved, the computer adjusted the loss coefficient to maintain the velocity. If the computer had to select a headloss coefficient less than 0.36, or the water level in the tank fell

below 56 ft above the test section horizontal centerline, the analysis was stopped. Initial results showed that the acceleration of flow in the test section was so extreme that cavitation took place. Therefore, an additional criterion had to be added to the analysis such that the loss coefficient was adjusted to the proper level in order to reduce the rate of increase of the test section velocity and correspondingly the reduction of test section static pressure. While the model was unstable due to the coarse time increment required, it appears that the time to establish flow will take approximately 18 seconds and the maximum velocity could be maintained for just over 100 seconds after the design velocity is achieved.

D. Test Section Boundary Layer Growth

A turbulent boundary layer will exist when the Reynolds number

$$R_x = \frac{Ux}{\nu}$$

where x = distance from leading edge of boundary layer and U = average free-stream velocity, equals approximate 10^6 . Applying the design value for velocity, the boundary layer becomes turbulent at a distance of

$$\frac{(10^6)(1.4 \times 10^{-5})}{(60)} = 0.235 \text{ ft} = 2\text{-}3/4\text{"}$$

from the origin of the boundary layer. The origin is an unknown entity; so for calculations it will be assumed that the boundary layer starts to grow at the beginning of the test section.

Using the above assumption of boundary layer origin in a computer program to calculate the boundary layer thickness on a flat plate, and assuming that the displacement thickness is $1/8$ the boundary layer thickness, the increase in diameter to maintain constant velocity is plotted in Fig. 6. For these computations, the boundary layer thickness was assumed to vary as

$$\delta = \frac{0.37x}{Re_x^{1/5}}$$

Plotted in Fig. 7 is a comparison of boundary layer displacement thickness and average axial velocity as flow proceeds through the test section if the test section diameter were to remain constant as proposed in Figs. 1 and 2.

E. Test Section Pressures

In order to obtain constant static pressure in the test section along the axial direction, the test section diameter must vary, of course, to compensate for boundary layer growth. Since the thickness of the boundary layer varies with the average test section velocity, it is necessary to select a representative average velocity and calculate the variation in diameter. In the case of this gravity flow facility, the selection of 60 fps was used and calculations have been previously presented in Fig. 6 as to the necessary diameter variation. With this modification, the pressure gradient in the test section should be close to zero; the static pressure does not vary along the streamwise component of direction.

High and low limits of static pressure in the test section are a function of the design selected. With the system demonstrated in Fig. 1 where the possibility exists to make the complete facility a closed loop (by arranging ducting so that air can exit the tail tank and enter the head tank as the water does the opposite), then the limits on high pressures are a structural constraint. That is, once the pressure is high enough throughout the system to avoid cavitation, increases in pressure do not affect the hydrodynamics of the facility and the structural limitations of pressure on the bulkheads become the governing factors. As indicated, the low limits of pressure would simply be the test section pressure that provides incipient cavitation.

With other proposed designs where there is no tail tank but rather a tail pool, the limits become more complex. Higher pressures in the test section can be achieved by applying pressure in the head tank (with air), but then this additional energy must be dissipated by the control valve at the exit. The characteristics of the control valve are unknown and, of course, the acoustic influence is of great importance. It is suggested that the high limit of pressure in the test section will be the point at which the energy dissipation of the control valve will transfer too great a proportion of that energy into the form of sound, rendering the facility useless. Lower levels of pressure in the designs providing tail pools would also require the manipulation of pressure in the head tank that could present problems to the acoustic quality of the facility.

In summary, the high and low limits of pressure in the test section is a function of the design selected. The proposal outlined in Fig. 1 presents the widest possible pressure range. A constant pressure of gradient equal to zero along the streamwise component of direction is possible by variance in the test section diameter in the flow direction.

F. Turbulence Management in the Gravity Flow Facility

In designing a possible turbulence management system, three factors must be considered in the mitigation of turbulent energy; (1) effects of the honeycomb, (2) effects of the stilling length and (3) effects of the contraction. Due to the large contraction ratio of the presently proposed design, it is the third factor of the above that should be addressed first.

Studies by Ramjee and Hussain [6] have experimentally demonstrated the invalidity of the theoretical effects of contractions on turbulence as

developed by Rikner and Tucker [7] and Batchelor and Proudman [8]. Applying the empirical results of Ramjee and Hassain for sudden contractions of varying area ratios of 11 to 100 (as displayed in Fig. 8) we can see that the ratio of existing relative turbulence to incoming relative turbulence is:

$$(u'/U)_e / (u'/U)_i = 0.08$$

$$(v'/U)_e / (v'/U)_i = 0.07$$

for a contraction ratio of 81.5, where u', v' = rms values of the longitudinal and lateral turbulent velocity fluctuations, respectively; U = mean velocity; subscript i = initial section value on the central streamwise axis at $0.4D$ upstream of the start of the contraction; subscript e = exit section value on the axis of the nozzle; and D = contraction inlet diameter.

The "turbulence reduction factor," η , of this contraction (borrowing nomenclature from Lumley and McMahon [9]) would be

$$\eta = 0.08^2 = 0.0064$$

for longitudinal turbulence, and a better (lower value) factor could be anticipated for the lateral turbulence reduction. However, for the sake of design, a value of $\eta = 0.0064$ will be utilized for all components of turbulence reduction, providing a small safety factor for discontinuities between the nozzle utilized by Ramjee and Hussain [6] and the final nozzle design applied to the gravity flow facility.

With the above selected turbulence reduction factor, we see that there must be a level of relative turbulence

$$(u'/U) \text{ and } (v'/U) = 1.25\%$$

at the nozzle entrance in order to achieve an acceptable level of relative turbulence at the contraction exit (test section entrance) of 0.1%. This degree of relative turbulence should be easily obtained with the proper honeycomb and stilling basin.

Next, a honeycomb was selected such that the turbulence entering the turbulence management system is attenuated to the 1.25% level at the contraction entrance. Since there was no specific information on the level of turbulence entering the honeycomb section, or the integral length scale of such turbulence, a honeycomb was chosen that would reduce an inflow turbulence level of 5% ($u'/U = 5\%$), at virtually any integral length scale, to a level of 1.25% upon exit. Utilizing the design technique of Lumley and McMahon [9] and the attached figures 9 and 10 from reference [9], a trial and error analysis was required, shifting between the two figures to optimize the solution. It was determined that a cell length " l " of 24 inches with a cell diameter (virtually equivalent to the distance across the flats on a honeycomb) of 0.7 inch would best suit this turbulence management system. Calculation of these parameters proceeded as follows:

(1) Calculate $\sqrt{\eta} \cdot \eta = (u'/U)_e^2 / (u'/U)_i^2$. Therefore $\sqrt{\eta}$ for the honeycomb that is required would be

$$\sqrt{\eta} = 1.25/5 = 0.25$$

(2) Select pressure-drop coefficient k . Since it was necessary (and prudent) to design the honeycomb independent of the turbulence integral length scale, selection of large k -values shown on Fig. 2 is required. It appears that the iso-reduction curve ($\sqrt{\eta}$ curves) for $\sqrt{\eta} = 0.25$ approaches $k = 1.5$ asymptotically. Therefore, a value of $k = 1.5$ was selected.

(3) Determine the length-to-diameter ratio. This is the ratio of the cell diameter (or distance across the flats of a hexagon) to the cell length in the direction of fluid flow. The length Reynolds number is

$$R_\ell = \frac{\ell U}{\nu} = \frac{(2')(0.7363 \text{ fps})}{(1.41 \times 10^{-5} \text{ ft}^2/\text{sec})}$$

$$R_\ell = 1.04 \times 10^5$$

Entering Fig. 10 with the length Reynolds number and the pressure drop coefficient $k = 1.5$, a length-to-diameter ratio of 33 was selected.

(4) Determine cell diameter. This is simply the cell length divided by the length-to-diameter ratio, or

$$D = \text{cell diameter} = 24"/33 = 0.727"$$

Any cell diameter of smaller size is of course acceptable, therefore the final design parameter was set at

$$D = 0.70 \text{ inches.}$$

The final aspect that was addressed was the stilling basin length. While this is critical in many other water tunnels, it is overshadowed by the effects of the honeycomb and the large contraction ratio of this gravity flow facility. Determination of the honeycomb parameters set specifications for length and cell diameter that can be easily achieved by industry while establishing a turbulence reduction factor that is adequate for obtaining the 0.1% turbulence level in the test section even without the benefit of turbulence decay in the stilling basin. However, the need still exists to eliminate the wakes in the trailing flow out of a honeycomb. Lumley and McMahon [9] insinuate that return to isotropy takes place at distances from the downstream face of the honeycomb greater than twenty cell diameters in their discussion on "combined fields." Research practice has normally selected 100 cell diameters as a safe distance

downstream from the honeycomb to guarantee the return in isotropy, which is believed to be very conservative.

A value of 50 cell diameters was selected for allowing the flow to return to isotropy. This means that a distance of three feet must exist between the downstream face of the honeycomb and the entrance to the contraction.

In summary, it is anticipated that a hexagonal cell honeycomb with a distance across of the flats of the hexagon less than or equal to 0.70 inches and a cell length greater than or equal to 24 inches placed in a stilling basin such that the downstream face of the honeycomb is at least three feet from the entrance of the contraction should produce a relative turbulence level in either the longitudinal or lateral direction (u'/U or v'/U) less than or equal to 0.1% in the test section, provided that the longitudinal turbulence entering the honeycomb is at a value of 5% ($u'/U = 0.05$) or less.

G. Suggested Component Modifications

1. Contraction

It is proposed that further study be carried out on the shape of the contraction. Of interest here is to insure that the contraction be free of any boundary layer separation at the inlet and cavitation-free at the exit. The length of the contraction should be as short as possible consistent with the other requirements to reduce boundary layer growth. A boundary shape defined by a sixth-order polynomial, fifth-order polynomial, or matched cubic equations should be investigated. These shapes, or any others, can readily be evaluated with a mathematical model developed for the Large Cavitation Channel. Boundary pressures as well as the velocity distribution can be obtained.

It may be desirable to divorce the contraction and the shape transition. The shape transition may be made upstream of the honeycomb, thereby reducing the tendency for any vortices for the corners to pass through the contraction into the test section.

2. Diffuser Transition

A smooth transition should be provided at the junction of the exit of the test section and the entrance to the diffuser. This is commonly done in water tunnels to reduce the possibility of separation and cavitation at that location. The transitional curve is preferably defined by a cubic equation, as a cubic satisfies the requirements of both zero slope and curvature at the entrance. The length of the transition can be taken as the diameter of the test section. The boundary pressure on this transition should be experimentally measured in a model.

III. ALTERNATE CONFIGURATION

Figures 11 and 12 picture the proposed revision and the following supportive comments apply:

A. Head Tank

The head tank in this case will consist of the same 36 foot diameter and the same provision for change in the free surface level (~ 40') as proposed by Wislicenus. Orifice studies have shown that adjacent upstream tank boundaries or tank-free surfaces have no influence on the efflux flow from an orifice in a tank wall provided these surfaces or boundaries are no closer to the orifice than about three jet diameters. That means that in this case the relation between the test section entrance dimensions or free surface positions are such that the tank may be considered the same as an infinite supply reservoir. It may be necessary to selectively place wall baffles on other anechoic surfaces within the tank to assist in improving turbulence resulting from tank filling operations. However, because of the small size of the tank filling jets (see Item F below) it is suggested that no baffles be included in the design until proven necessary by model or full-scale trials. It is also suggested that no anti-vortex device be used at the free surface above the test section entry. Effluent openings of this kind are usually fitted with such devices but this practice stems from experience with steady-state discharges. However, SAFHL blow-down tank studies for NASA (Memos 138, 160) showed that the short time spans employed in blow-down tanks are not sufficient to permit establishment of surface vortices. It should be noted that the revised head tank is substantially taller than that proposed by Wislicenus. This is not expected to incur extra cost because the simpler tall tank can probably be located on grade whereas the short tank requires supporting framing. Care should be taken to see that condensation on the inside of the tank roof and drainage from tank walls or baffles does not drip on the free water surface. Dripping may prove to be an annoying noise source.

B. Test Section

The test section considered here is taken the same as that proposed by Wislicenus. However, the attached entrance contraction and the exit transition are different. In addition to the change in the contraction piece, it is recommended that the upstream portion of the test section be inherently attached to a removable panel which can be bolted to the wall of the head tank. This would permit convenient changing to alternate test section configurations without modification of the basic head tank. Elimination of the vaned elbow, honeycomb, and large contraction in the revised design should provide substantial fabrication savings, reduction of flow, head loss, and elimination of virtually all of the flow boundary layer formerly developed upstream of the test section. This should materially assist in silencing the approach flow system. The test section-diffuser transition is discussed in Item D below.

C. Entrance Contraction

In view of the proposed tank revisions (Item A above) which provide an infinite tank approach system, the contraction entrance to the test section can be of very small size and yet provide a flow of exceptionally high quality (minimum turbulence and inflow boundary layer). A variety of relatively inexpensive and effective entrance configurations can be conceived and no fix on this form will be suggested at this time.

D. Downstream Diffuser

The juncture between the downstream end of the test section and the beginning of the conical diffuser should include a boundary transition curve. The exact nature of the transition curve, including its low pressure dip, can be established by design information available in various reports of the earlier water tunnel studies conducted at SAFHL for DTMB and of NSRDC. Care should be taken to see that the tunnel axial pressure gradient for maximum test section velocity at minimum head tank stage, including the low pressure dip inherent to the selected boundary transition curve, remains comfortably above that which leads to cavitation.

Normally a 5° conical diffuser should be free of boundary layer separation. However, data from a 5° conical diffuser of only 12 diameters length showed significant separation (SAFHL Tech. Paper 9-B, Fig. 28) about 8 diameters downstream of the diffuser entrance. The abnormality found in these data was not wholly explained but was attributed to an asymmetry imposed on the diffuser flow by improper setting of the vanes in the elbow. Since the very long length of the proposed diffuser (33 diameters) probably provides even greater sensitivity to any asymmetry in the elbow or headloss controller, a gravity model study should be used to establish the flow separation sensitivity to symmetry of flow. Noise should be measured for the test conditions and a noise tolerance established. The gate valves of the controller-Head Dissipator could conceivably be fined tuned to adjust for any flow asymmetries induced by the vaned elbow.

E. Controller and Head Dissipator

This component, which is to be taken directly from the Wislicenus design, was not adequately described. Since it is evidently the result of considerable analysis, no attempt will be made to discuss it here or to offer an alternate design.

F. Short Diffuser

The short inlet diffuser shown in the revision Sketch would be designed in general conformance with a similar elbow-diffuser configuration already designed and tested at SAFHL (SAF Memo M-134, Fig. 27) as shown in Fig. 12. This diffuser which has a 90° included cone angle, uses four stages of perforated resistance plate to expand the flow. The new design would be very similar to that of Fig. 12 but would employ relatively large perforation holes in the first three stages and a fourth stage with finer holes, say 1/8 inch diameter. The resulting jets introduced into the head tank during filling would be very great in number but very small in size. These jets would generate very small scale tur-

bulence with a short eddy-decay life. It is anticipated that the turn-around time between tests could be made quite brief with this system.

G. Vaned Elbow

This elbow, like the diffuser of Item F, is described in Fig. 12. It can be readily sized to fit the selected pump discharge diameter or increased in size if a pump diffuser (see Item J below) is employed. No problems are anticipated with this unit.

H. Pump Discharge Line

This line should be sized to match the needs of the pump and the short diffuser. No special flow problems are anticipated with this component.

I. Pump Diffuser

This diffuser may or may not be needed, depending on the match that is made between the pump size and the inlet size preferred for the design of the short diffuser of Item F.

J. Refill Pump

The refill pump would be taken from the design of Wislicenus. It is assumed that a valve will be used in the pump discharge line to isolate the head tank from the tank containing the controller-head dissipator component during the test blowdown.

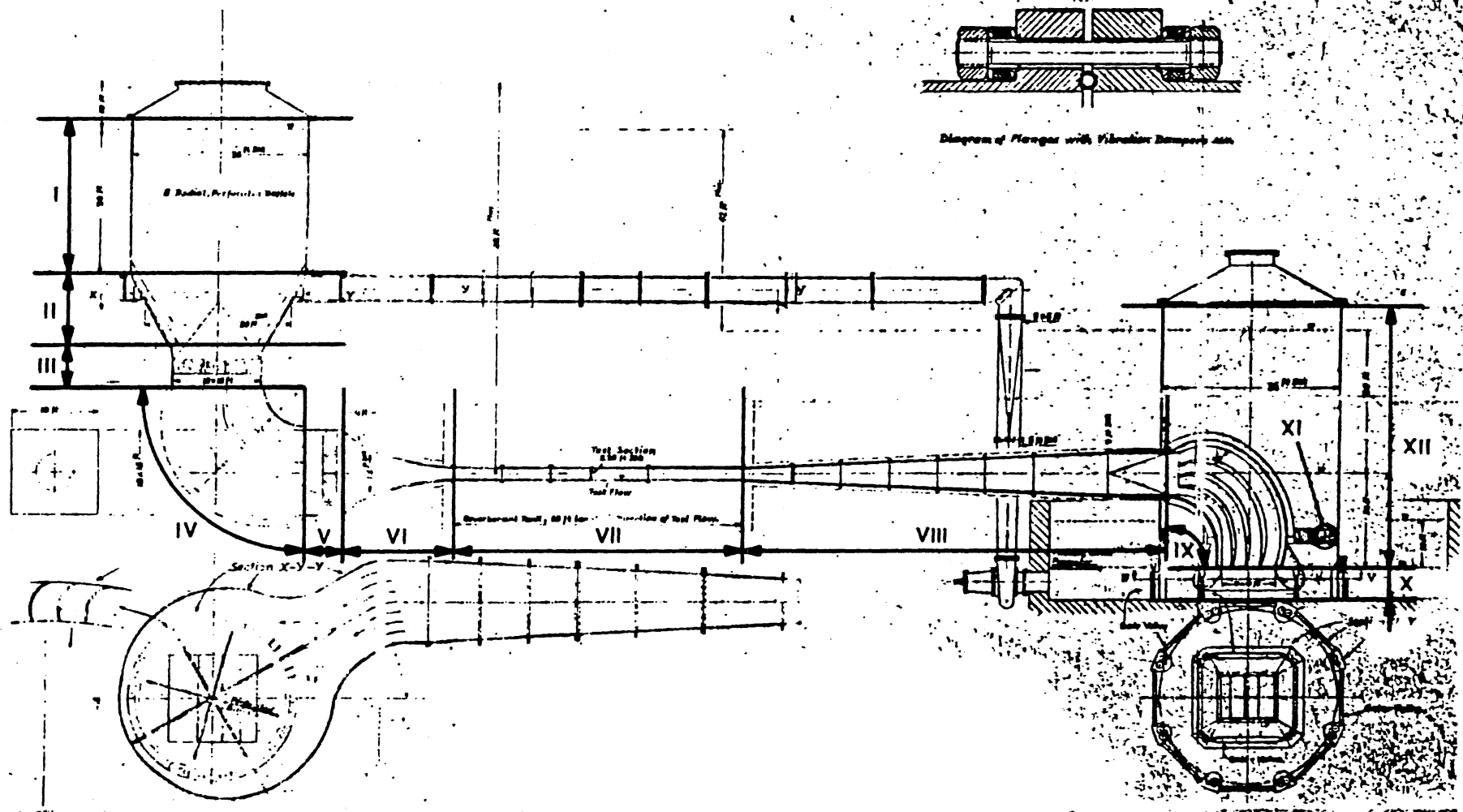


Fig. 1. Hydroacoustic gravity flow facility for ship silencing laboratory with sound-absorbing corner vane systems. November 26, 1982 George F. Wislicenus.

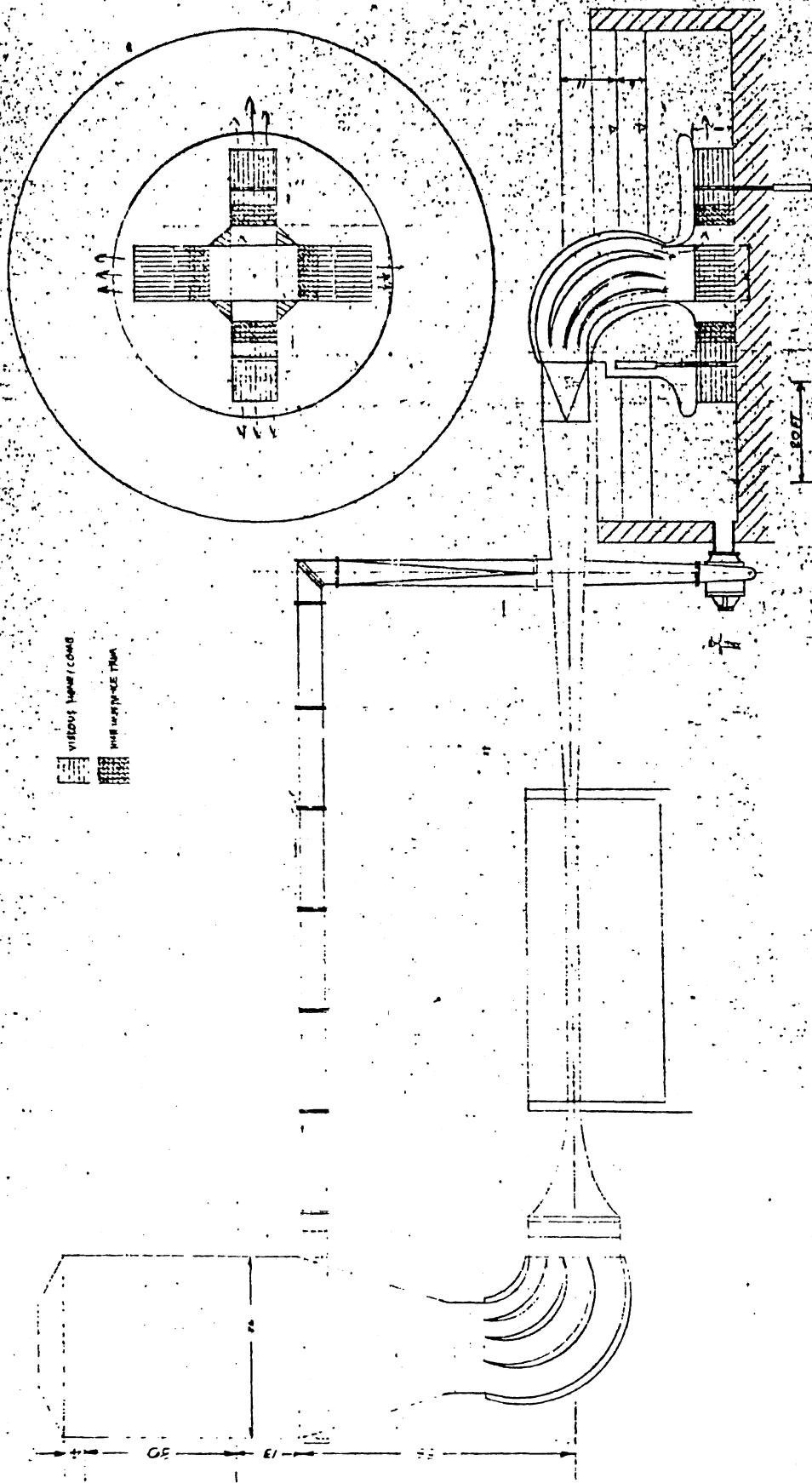
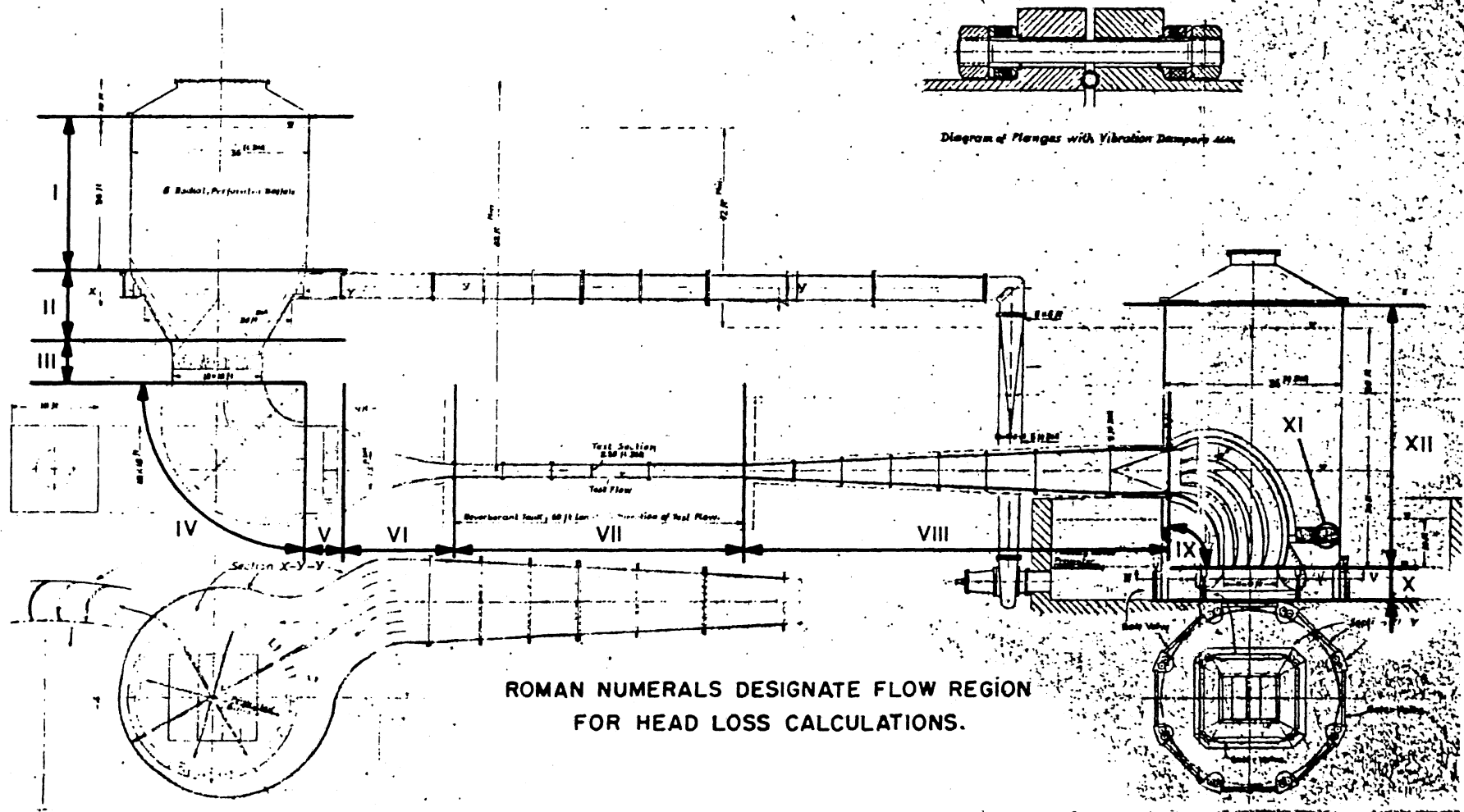


Fig. 2. Alternate gravity flow facility design.



ROMAN NUMERALS DESIGNATE FLOW REGION FOR HEAD LOSS CALCULATIONS.

Fig. 3. Definition of flow regions in the gravity flow facility.

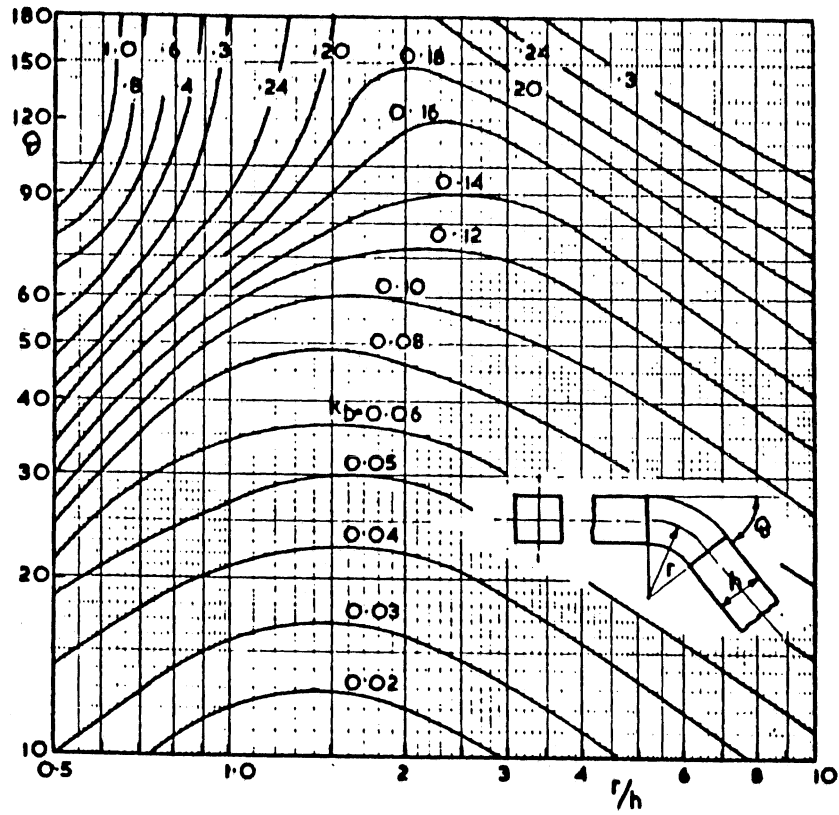


Fig. 4. Loss coefficient k for square cross-section bends. From Miller [1], Fig. 3.2.2.

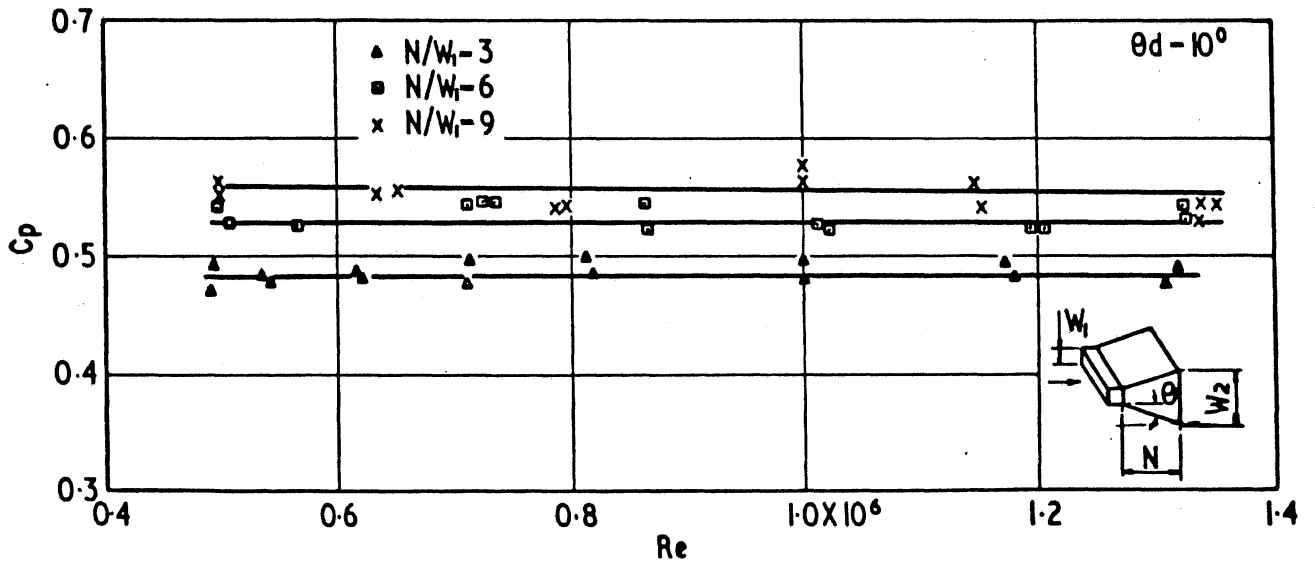
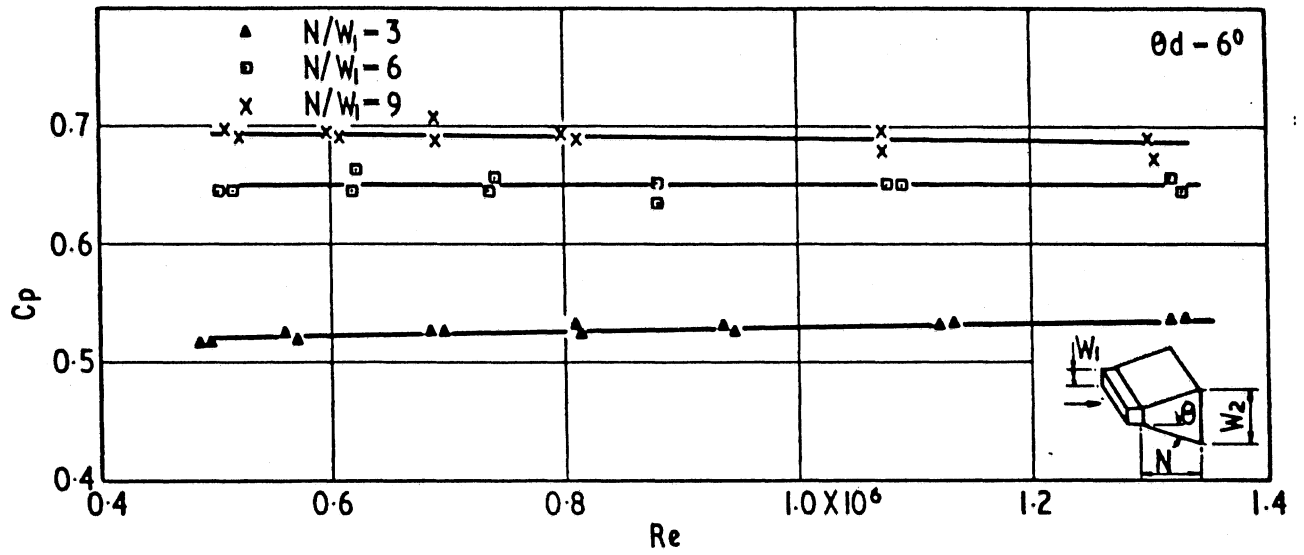
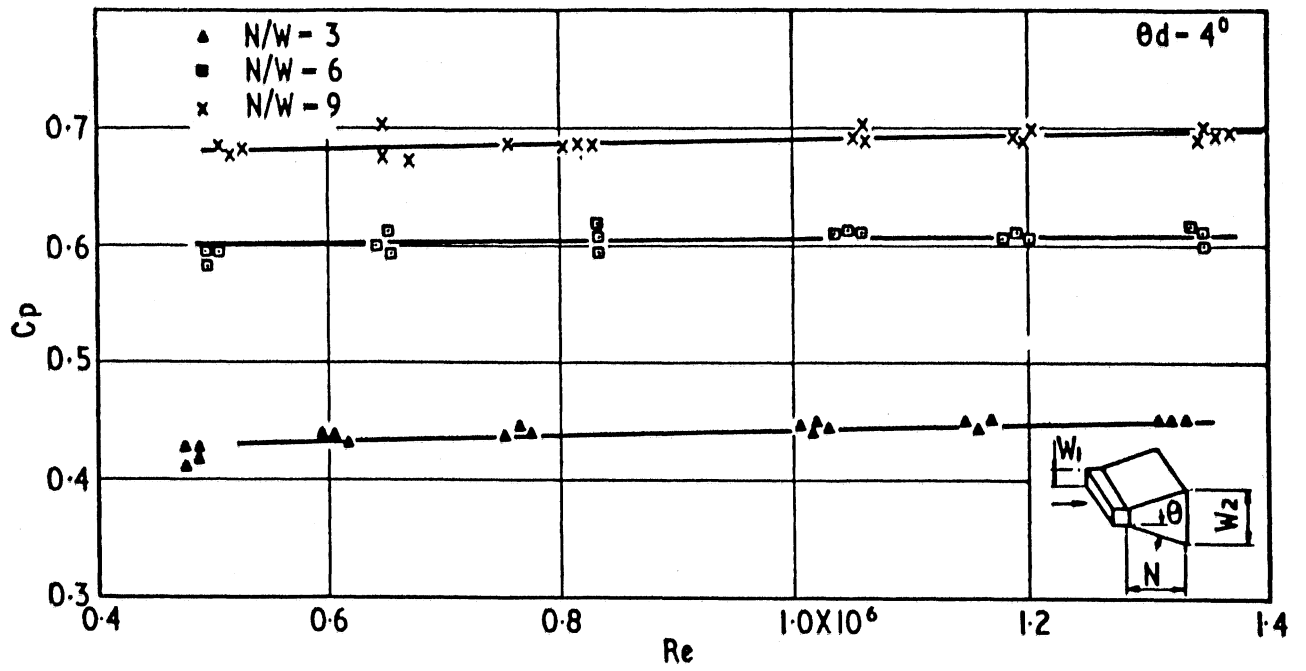


Fig. 5. Pressure recoveries - rectangular diffuser ($AR = 2$, $L/D_1 = 30$)-free discharge
From Miller [1], Fig. 61.

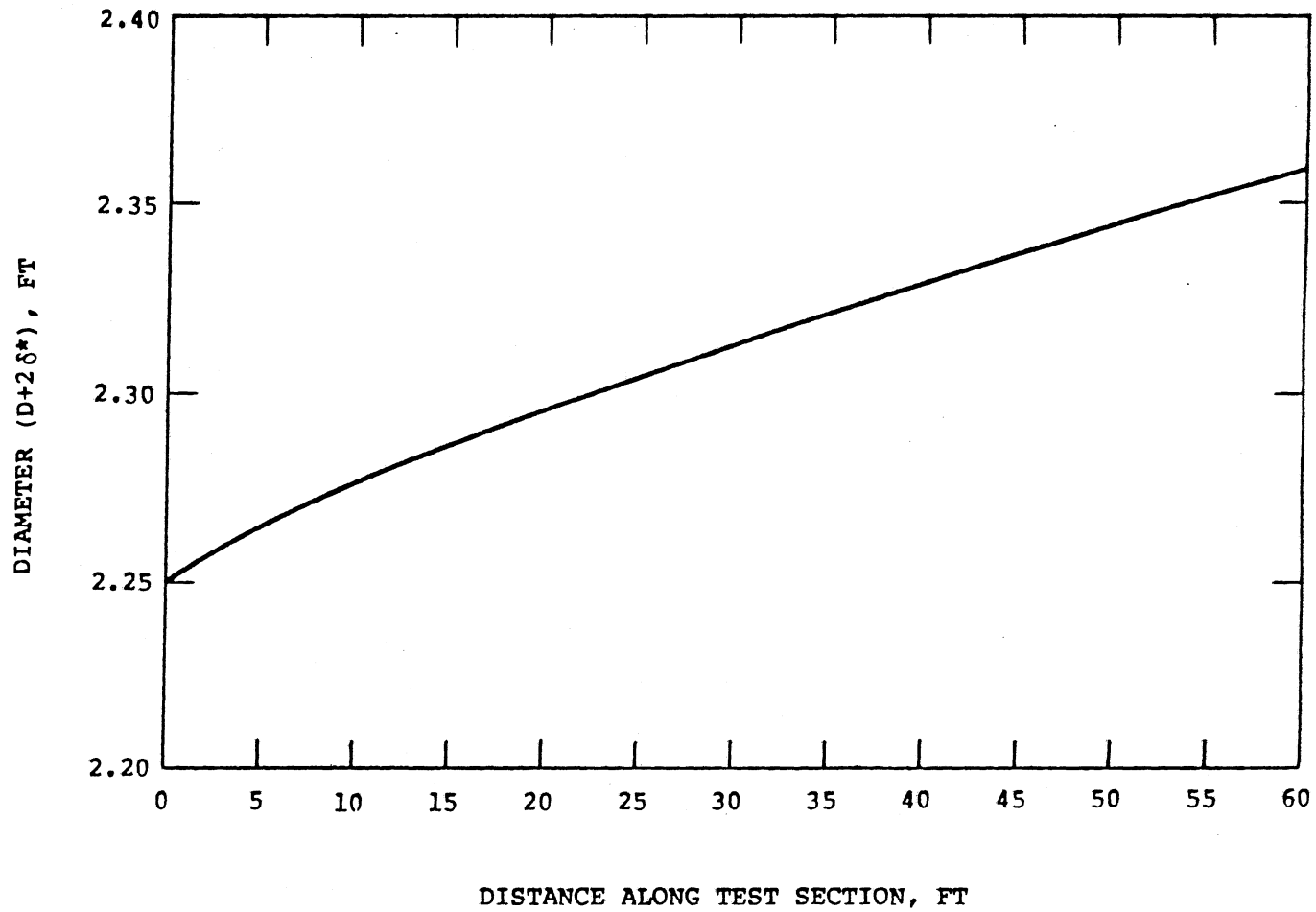


Fig. 6. Variation of test section diameter to maintain constant axial velocity.

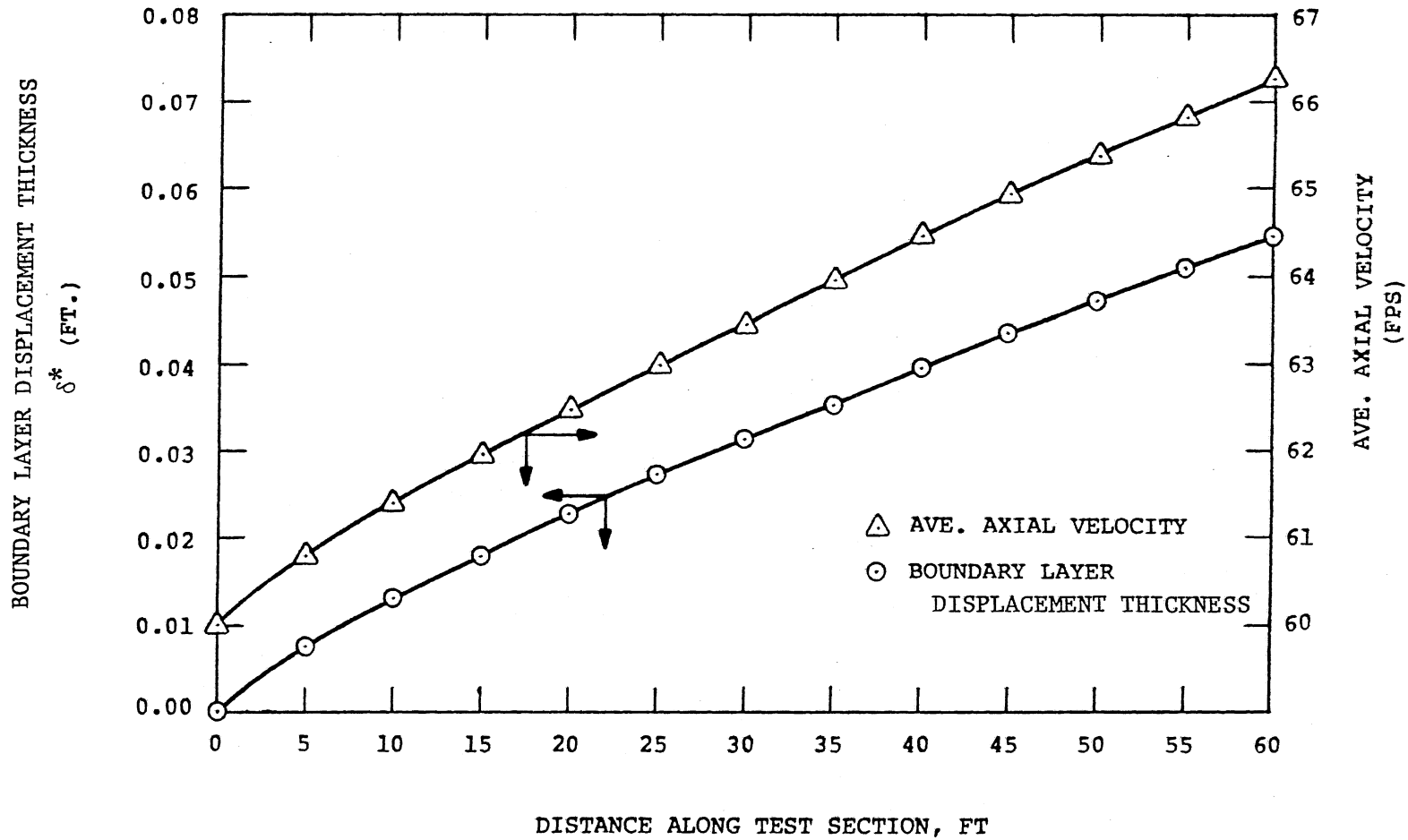


Fig. 7. Boundary layer displacement thickness and average axial velocity in gravity flow facility with constant test section cross-sectional area.

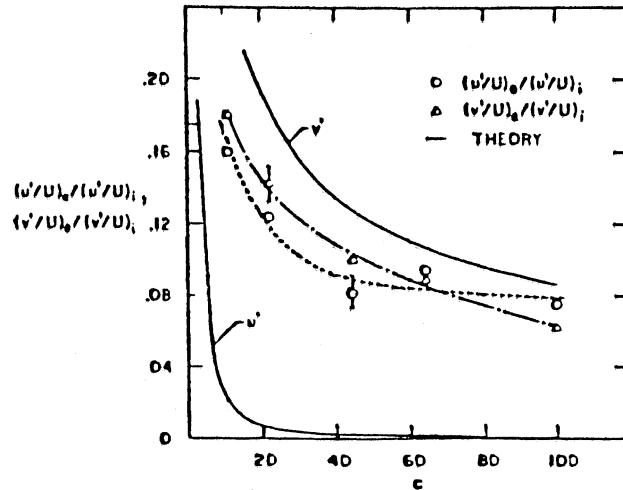


Fig. 8. Ratios of exit to initial turbulence intensities for different contraction ratios, c . From Ramjee and Hussian [6].

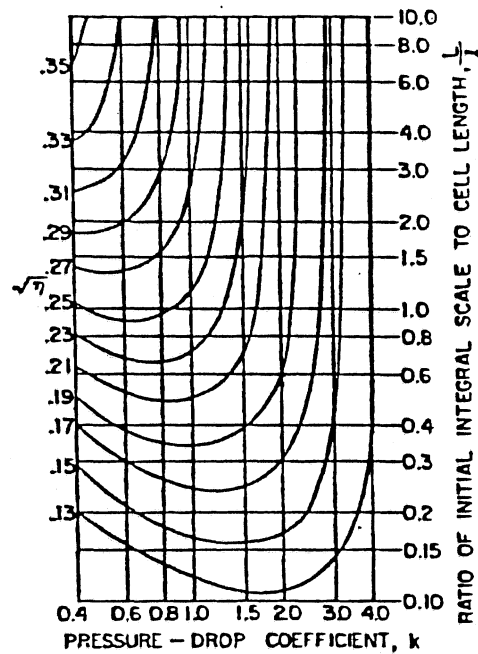


Fig. 9. Isoreduction contours as a function of pressure-drop coefficient and ratio of integral scale of initial turbulence to cell length. From Lumley and McMahon [9].

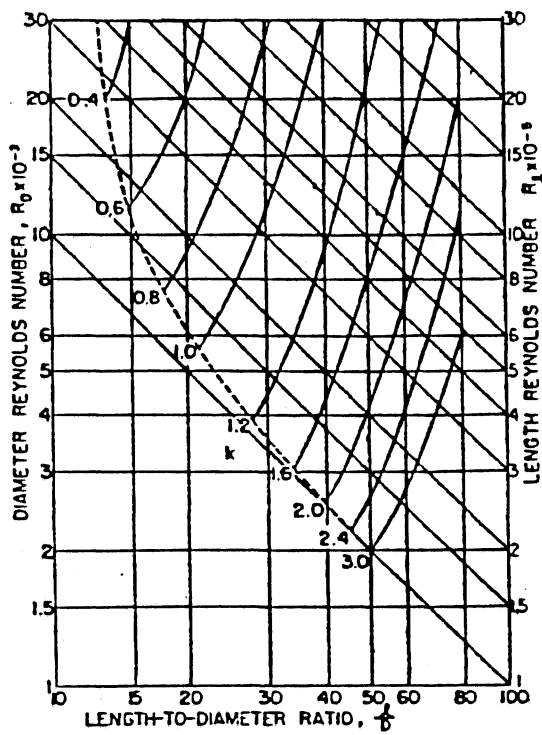


Fig. 10. Pressure-drop coefficient and length Reynolds number as a function of diameter Reynolds number and length-to-diameter ratio. Flow is fully developed above and to the right of the dashed line. From Lumley and McMahon [9].

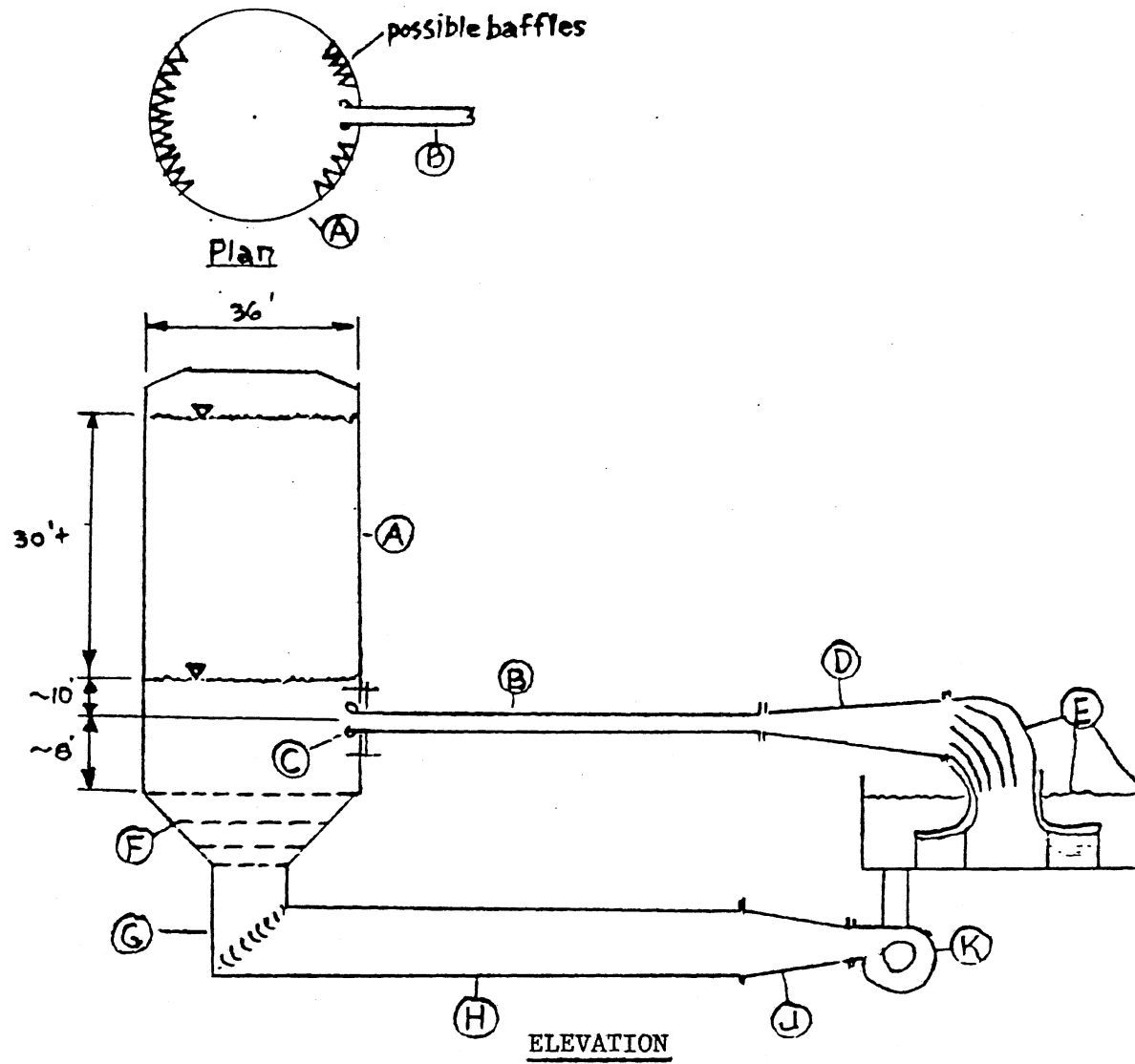


Fig. 11. Proposed revision of hydroacoustic facility

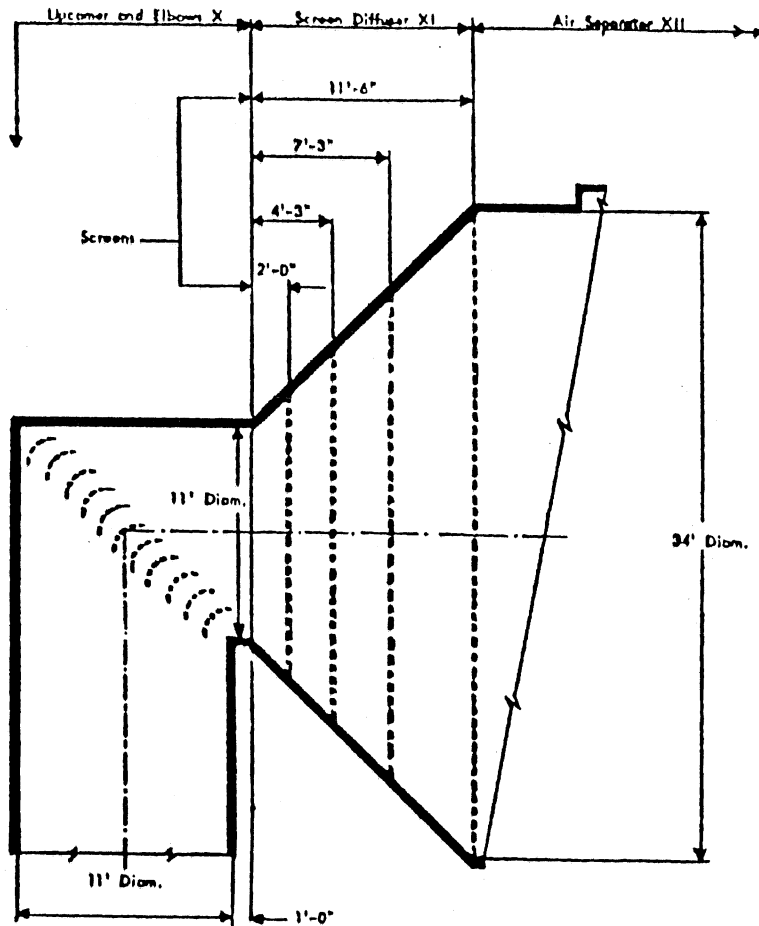


Fig. 12. The screen diffuser configuration (all dimensions relate to prototype inside flow surfaces). Taken from SAFHL External Memorandum M-134.

REFERENCES

1. Miller, Donald S., "Internal Flow, A Guide to Losses in Pipe and Duct Systems," British Hydromechanics Research Association, 1971.
2. Ripken, J. F., "Design Studies for a Closed-Jet Water Tunnel," St. Anthony Falls Hydraulic Laboratory, University of Minnesota, Technical Report No. 9, Series B, August, 1951.
3. Schlichting, H., Boundary Layer Theory, Seventh Ed., McGraw-Hill, New York, 1979.
4. Idel'chik, Handbook of Hydraulic Resistance, Coefficients of Local Resistance and of Friction, AEC-TR-6630, NTIS, 1960.
5. McDonald, A. T. and Fox R. W., "Incompressible Flow in Conical Diffusers," Purdue Research Foundation, Tech. Report No. 1, U. S. Dept. of Defense Unclassified AD 448505, ARO(D), Project No. 4332 (463), Sept., 1964.
6. Ramjee, V. and Hussain, A.K.M.F., "Influence of the Axisymmetric Contraction Ratio on Free-Stream Turbulence," Journal Fluids Engineering, ASME, September, 1976, pp. 506-515.
7. Ribner, H. S. and Tucker, M., "Spectrum of Turbulence in a Contracting Stream," NACA Report, Nol. 1113, 1953.
8. Batchelor, G. K. and Proudman, I., "The Effect of Rapid Distortion of a Fluid in Turbulent Motion," Quarterly Journal Mechanics and Applied Mechanics, Vol. 7, 1954, pp. 83-103.
9. Lumley, J. L. and McMahon, J. F., "Reducing Water Tunnel Turbulence by Means of a Honeycomb," ASME Fluids Engineering Division, Paper No. 67-FE-5, February, 1967.